MULTI-OBJECTIVE TOPOLOGY OPTIMIZATION FOR TRABECULAR BONE-LIKE STRUCTURE: ROLE OF STABILITY AND SURFACE AREA

BY

DARIN PEETZ

THESIS

Submitted in partial fulfillment of the requirements
for the degree of Master of Science in Civil Engineering
in the Graduate College of the
University of Illinois at Urbana-Champaign, 2016

Urbana, Illinois

Adviser:

Professor Ahmed E. Elbanna

ABSTRACT

We apply a multi-objective topology optimization framework to examine the evolution of structural complexity in a vertebral body under the competing requirements of compliance, surface area, and buckling stability. We use a classical rectangular plate model with uniform external load to demonstrate that the complexity of the resulting structure is driven by the optimization criteria rather than a specific domain geometry or loading pattern. We show that compliance minimization alone is incapable of replicating the intricate structure of the trabecular bone. Inclusion of surface area maximization is necessary for reducing member sizes and generating a sufficient number of voids, but only with the addition of the stability considerations do significant non-vertical features in the trabecular structure start to develop, giving the full sponge-like architecture. In addition, our multi-objective approach provides the flexibility to determine the relative role of the different objectives without the need to specify preset values for constraint functions that may not be directly available. We discuss the implications of our work, particularly in the realm of biomimicry.

To my wife, for making sure I don't starve.

ACKNOWLEDGMENTS

A. E. Elbanna acknowledges support from the National Science Foundation NSF CMMI 251005. Data is available by contacting the corresponding author.

TABLE OF CONTENTS

LIST OF FIGURES

CHAPTER 1

INTRODUCTION

In the late 1800s, Julius Wolff first noted the similarities between the work of Meyer [2] in describing the trabecular structure within human proximal femur and the work of Culmann [3] in describing the principle stress patterns in a curved bar. Realizing the connections between these structures, Wolff hypothesized that trabecular bone naturally adapts to the present stress trajectories and is thus a self-optimizing material. This theory, now known as Wolffs law [4], has more recently been explored using topology optimization in an attempt to recreate these structures. In particular, some researchers have been able to generate 2D and 3D models that closely resemble the trabecular bone in the proximal femur using topology optimization [5, 6]. This success both reaffirms the theories put forth by Wolff and offers new insight into structural design. In these studies, minimization of compliance is frequently used as an objective in combination with a constraint on volume and surface area of the pores (measured as total perimeter in the 2D case). In this scheme, perimeter is constrained to have a minimum value in order to create a larger number of pores in the structure, as opposed to the more typical procedure of reducing perimeter in order to prevent oscillating material designs (checkerboarding) [7].

While this scheme produces good approximations of bone architectures in the case of the femur, it overlooks the investigation of the stability in the optimized structure. In domains where the load is primarily in one direction, such as the vertebral body [8], the optimization will generally produce long members aligned with the direction of loading that may be prone to instability. In this paper, we have thus extended the minimization of compliance-maximization of perimeter scheme to include structural stability in order to produce a more complex structure as seen in the vertebral body (Figure1.1).

Few previous studies have incorporated structural stability in relation to topology optimization, partially due to its relatively high computational cost.

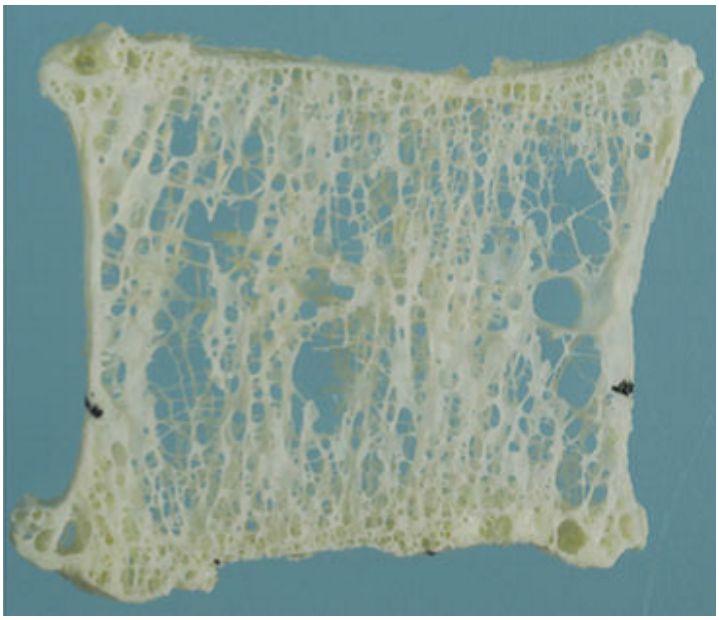

Figure 1.1: Sagittal cross-section of vertebral body [1].

Early papers by Neves et al. [9] and Min and Kikuchi [10] introduced methods to account for linear buckling behavior in topology optimization. Cheng et al. [11] used this formulation in the design of column-like linear elastic structures for stability. Bian and Sui [12] studied the effects of using buckling and displacements as constraints. More recently, Browne et al. [13] proposed a novel method to overcome the enormous cost of the buckling formulation by using a binary optimization method to reduce the number of iterations (the Fast Binary Descent Method) and requiring fewer sensitivity calculations. Lindgaard and Dahl [14] have expanded the formulation to include nonlinear buckling theory. The book by Bendse and Sigmund [15] also remains a valuable resource on the topic.

In this paper we present a multi-objective topology optimization approach for the problem of vertebral architecture. We consider the following objectives: compliance, perimeter, and buckling strength, in addition to a constraint on the volume fraction. The inclusion of compliance and volume will, as usual, ensure that the structure is one that efficiently reduces deformation when subjected to an external load. The perimeter function forces the structure to maximize the number of pore spaces, a biologically motivated objective, particularly when referring to trabecular bone. Finally, the buckling load function will prevent the increasingly perforated structure from becom-

ing unstable. Several papers ([5, 6, 16] to name a few) have demonstrated success in recreating trabecular-like structures using compliance minimization with perimeter and volume constraints, particularly in the proximal femur. However, we will demonstrate that stability plays an important role, particularly in the vertebral body. We will also discuss the benefits in treating perimeter and stability as additional objectives rather than constraints in the formulation. Combining all of the functions (including volume) into a single objective, without any conventional constraints, is a possible subject of future work.

CHAPTER 2

OPTIMIZATION FRAMEWORK

Topology optimization is a mathematical approach to construct the material layout within a given design space that meets a prescribed set of performance measures for a given set of boundary conditions. To that end, a set of functions are introduced to define the objectives to be optimized along with a set of constraints that the optimal solution must satisfy. This is done by discretizing the domain into a mesh and assigning each element a density between 0 (void) and 1 (solid material). A finite element analysis is then performed for the proposed design and the results (stresses and displacements) are used in the prescribed set of functions to evaluate the objectives. The design is then updated with either a gradient-based optimizer and associated sensitivity analysis or using a non-gradient based approaches such as a genetic algorithm ([17] and references therein), and the new values of the elements density are passed to the finite element analysis. This iterative process is repeated until the objective functions converge to their optimal values.

We chose to discretize the design space using bilinear quadrilateral elements. Since this is a low order element, the optimal solution may exhibit checkerboarding [18]. This phenomenon occurs due to the difficulty in accurately representing bending modes with low order elements, causing elements connected by only a node to lock together rather than rotating freely about the node. This locking leads to material designs where contiguous elements have densities that vary in a periodic fashion, similar to the design of a checkerboard. While a real structure with such a design would have very low stiffness, the element locking gives the finite element model a stiffness nearly equal to that of a solid material. This modeling error will lead to designs that have low robustness and are nearly impossible to manufacture. To prevent the occurrence of checkerboards and overcome element locking, we include a linear density filter to interpolate design values to element densities [19, 20].

This filter is defined by:

$$\tilde{\rho}_i = \sum_j w_{ij} \rho_j \tag{2.1}$$

with weight factor, w_{ij}, defined by:

$$w_{ij} = \begin{cases} \frac{R - d(i,j)}{\sum_{k \in N_i} R - d(i,k)} & \text{if} j \in N_i \\ 0 & \text{otherwise} \end{cases} \tag{2.2}$$

The value of R, commonly known as the filter radius, describes a circular neighborhood for the element, $N_i = \{j : d(i,j) \leq R\}$, where $d(i,j)$ defines the distance between elements i and j. The weight factor is greater than zero for elements within the neighborhood of element i and zero for all other elements. It is common to ensure that no density is added or lost from the domain when all design variables are equal. This is done by enforcing the condition:

$$\sum_j w_{ij} = 1, \quad \forall i \tag{2.3}$$

and we follow this in the current manuscript.

To ensure that the optimizer converges to a binary design (density values of 0 or 1) the intermediate density values are penalized, using the solid isotropic material with penalization model (SIMP) [21, 22]:

$$\begin{aligned} E_e &= \varepsilon + (1 - \varepsilon)\tilde{\rho}_e^p E_0 \\ V_e &= \tilde{\rho}_e \end{aligned} \tag{2.4}$$

where $p \geq 1$ is a penalty factor, ε is a small number (1e-4) to keep the stiffness matrix from becoming singular as $\rho_e \to 0$, and E_0 is a reference element stiffness corresponding to the solid material. In our case, we also use a continuation approach [23] where we incrementally increase the penalty factor from 1 to 4 to improve the convexity of the design space. It is possible to perform the entire optimization problem with a single penalty value, for example using a penalty of 3. However, destroying convexity of the problem makes it extremely unlikely to converge to a global minimum. Using the

continuation approach also does not guarantee a local optimum, but the initial optimization steps taken in the convex domain should lead to a design with a better local optimum (although this is again not guaranteed).

To calculate the design update we make use the Method of Moving Asymptotes (MMA) [24]. There is a debate in the literature as to the relative merit of gradient-based and non-gradient-based optimizers, but it is the opinion of the authors that gradient-based optimizers are better suited for the problem of interest in this paper due to their much lower cost, since analytical expressions for the relevant design sensitivities are readily available. In addition, gradient-based optimizers require fewer function evaluations, which is very important considering the high cost of the eigenvalue problem, which we will discuss later. As such, we have elected to use MMA in our work due to its low computational cost, ease of implementation (the user need only supply constraint values and design sensitivities), and flexibility in handling a wide variety of objective and constraint functions.

CHAPTER 3

MODEL SETUP

3.1 Domain and Boundary Conditions

For all of the cases presented here we have modeled the vertebral body as a rectangular domain with uniform rectangular elements. This plate model has been repeatedly examined in the context of bone remodeling [25, 26, 27]. The regularity also gives us a better insight into the influence of each of the optimizer functions independent of the influence of complex geometrical features. Considerations of more complicated boundary geometries will be part of a future investigation.

For boundary conditions, we have chosen an idealized case with equal uniformly distributed load at the top and bottom of the domain, consistent with the loading conditions in a healthy spine. Across the bottom of the domain we also add very compliant springs (less than 1% of the element stiffness), to eliminate rigid body modes Figure 3.1. This closely resembles the case of vertebral bone as there are no true rigid connections (the entire vertebral body can move freely in any direction). However, the forces applied to the body are in equilibrium and the surrounding tissue prevents the bone from moving out of place, meaning that any displacements are due to internal strains (no rigid body modes). This set of boundary conditions facilitates investigating the effect of different objective/constraint functions on the topology of the structure independent of the additional complexities introduced by non-uniform loading and support conditions.

All of the examples in the Results section use a 100x100 element mesh. The solid material is assumed to be isotropic linear elastic with a Poissons ratio of 0.3 and Youngs Modulus of 15 GPa (although the modulus value is unimportant here as the FEM problem and all objective/constraint functions are linear). As an initial condition, we assign uniform density to each element

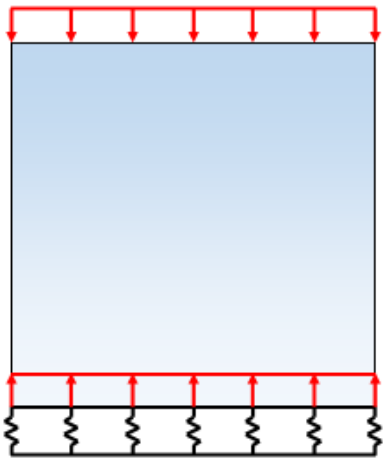

Figure 3.1: Domain and Boundary Conditions used in all cases. The domain is square of unit side length. The loading is assumed to be uniformly distributed along the top and bottom edges. Compliant springs are added to the bottom of the domain to prevent singularity of the stiffness matrix while still allowing for deformations along that edge.

in the mesh consistent with the volume constraint. The filter radius in all cases is set to 1.5 times the largest dimension of the elements.

3.2 Functions

In this paper we use a method that effectively combines multiple functions, such as compliance, perimeter, and critical buckling load, in the presence of a constraint on volume fraction. Each of these functions relates to a biological purpose that trabecular bone must serve. We combine these functions using a weighted sum multi-objective formulation.

3.2.1 Compliance and Volume

We begin by looking at the most commonly referenced optimization problem, compliance minimization with a volume constraint [28]. This simple formulation creates an efficient structure that minimizes displacements in response to the applied loading. The problem is formulated as:

$$\begin{aligned} \min_{\rho} \quad & f = \mathbf{f}^T \mathbf{u} \\ \text{s.t.} \quad & \frac{1}{n_{el}} \sum_{e=1}^{n_{el}} \rho_e A_e \leq V \end{aligned} \tag{3.1}$$

where $\mathbf{f}$ is the vector of discrete loads applied at all the nodes in the mesh, $\mathbf{u}$ is the vector of displacements of all of the nodes as determined by solving $\mathbf{Ku} = \mathbf{f}$, ρ_e is the density of element e, V is the desired maximum volume fraction, and n_{el} is the total number of elements in the discretization. For a uniform mesh the volume function simplifies to the average of all element densities:

$$\frac{A}{n_{el}} \sum_{e=1}^{n_{el}} \rho_e \leq V \tag{3.2}$$

While a constraint on volume fraction is very common in topology optimization, and has been applied successfully in other attempts to mimic trabecular structure, we argue that the concept of a constraint is difficult to motivate biologically. The volume of trabecular bone would need to readily adapt for a variety of factors including nutrient loss, change in loads, injury, etc. With this idea in mind, we will later demonstrate the validity of including the volume fraction as an objective, rather than a constraint (see Appendix). However, for the results reported in the body of this paper we keep the volume as a constraint.

3.2.2 Perimeter

In many biological structures such as bone, surface area of the structure appears to be as important as stiffness. This is because several biological functions, such as nutrition intake, mineralization and self-healing, depend on the surface area of the structure available for interaction with the surrounding environment [29, 30]. To account for this in the formulation, a constraint on surface area (or perimeter in the 2D case) was introduced by Jang and Kim [6]. For a uniform rectangular mesh, the value of the perimeter function is formulated as:

$$P = \sum_{j=0}^{n_y} \sum_{i=1}^{n_x} h_y |\rho_{ij} - \rho_{i-1,j}| + \sum_{j=1}^{n_y} \sum_{i=0}^{n_x} h_x |\rho_{ij} - \rho_{i,j-1}| \tag{3.3}$$

where n_x and n_y are the number of elements in the x and y-dimensions and h_x and h_y are the dimensions of those elements in the x and y-dimensions, respectively. The above expression only applies to a rectangular mesh of elements, which is used here, but it is easily generalizable to irregular meshes, if needed. In our formulation, we use this perimeter formulation as an additional objective with compliance and/or stability rather than a constraint. A more detailed explanation for making this change is available in the Discussion section.

Both the volume and the perimeter functions are normalized to relieve mesh dependencies. The volume function may be conceptualized as the volume of the structure divided by the maximum possible volume:

$$\frac{\sum_{e=1}^{n_{el}} \rho_e A_e}{\sum_{e=1}^{n_{el}} A_e} \tag{3.4}$$

Similarly, the perimeter function may be conceptualized as the perimeter in the structure divided by the maximum possible perimeter. The maximum possible perimeter is inherently mesh dependent, but for a regular mesh of quadrilateral elements the maximum perimeter occurs when the structure is a checkerboard. In this case the perimeter value is equal to the total number of elements times the sum of the element dimensions:

$$P_{max} = n_x n_y (h_x + h_y) = n_{el}(h_x + h_y) \tag{3.5}$$

Thus, the normalized perimeter function that is used in this manuscript takes the form:

$$\frac{\sum_{j=0}^{n_y} \sum_{i=1}^{n_x} h_y |\rho_{ij} - \rho_{i-1,j}| + \sum_{j=1}^{n_y} \sum_{i=0}^{n_x} h_x |\rho_{ij} - \rho_{i,j-1}|}{n_{el}(h_x + h_y)} \tag{3.6}$$

3.2.3 Stability

Depending on the domain and boundary conditions used in the optimization problem, the results obtained through only the compliance, perimeter and volume functions may correspond to an unstable structure. This may happen for example when the perimeter function is high and the volume fraction is low, resulting in thin and elongated elements. The structure may become even more vulnerable, from a stability point of view, if the loading is uniaxial and all the members align in the same direction. To alleviate this potential instability, we have included a calculation of the critical buckling load in accordance with small strain theory. The critical buckling loads for a given structure are calculated using the formula [15]:

$$(\mathbf{K}_\sigma \mathbf{u} - \lambda_i \mathbf{K})\phi_i = \mathbf{0} \tag{3.7}$$

Where $\mathbf{K}_\sigma$ is the stress stiffness matrix (also referred to as the geometric stiffness matrix) which uses the displacements obtained from the linear problem $\mathbf{Ku} = \mathbf{f}$, λ_i is the inverse of critical load i, and ϕ is the eigenvector describing buckling mode i. The element stress stiffness matrix is formulated as:

$$\mathbf{k}_\sigma = E_\sigma \int_{\Omega_e} \mathbf{G}^T \mathbf{S} \mathbf{G} dv \tag{3.8}$$

Where, for bilinear quadrilateral elements as an example:

$$\mathbf{G} = \begin{bmatrix} \frac{\partial N_1}{\partial x} & 0 & \frac{\partial N_2}{\partial x} & 0 & \frac{\partial N_3}{\partial x} & 0 & \frac{\partial N_4}{\partial x} & 0 \\ \frac{\partial N_1}{\partial y} & 0 & \frac{\partial N_2}{\partial y} & 0 & \frac{\partial N_3}{\partial y} & 0 & \frac{\partial N_4}{\partial y} & 0 \\ 0 & \frac{\partial N_1}{\partial x} & 0 & \frac{\partial N_2}{\partial x} & 0 & \frac{\partial N_3}{\partial x} & 0 & \frac{\partial N_4}{\partial x} \\ 0 & \frac{\partial N_1}{\partial y} & 0 & \frac{\partial N_2}{\partial y} & 0 & \frac{\partial N_3}{\partial y} & 0 & \frac{\partial N_4}{\partial y} \end{bmatrix} \tag{3.9}$$

$$\mathbf{S} = \begin{bmatrix} \sigma & \mathbf{0} \\ \mathbf{0} & \sigma \end{bmatrix} \tag{3.10}$$

$$\sigma = \begin{bmatrix} \sigma_{xx} & \sigma_{xy} \\ \sigma_{xy} & \sigma_{yy} \end{bmatrix} \tag{3.11}$$

N_i are the nodal shape functions and x and y are the global coordinates of the elements. The construction of $\mathbf{K}_\sigma$ is described in more detail in [31].

Assembly of the local stress stiffness matrices to the global stress stiffness matrix is identical to the assembly of the stiffness matrix. However, the

interpolation of the element stiffness is done differently for the stress stiffness matrix than it is for the material stiffness matrix. As opposed to the formulation in (4), the element stiffness is now formulated as:

$$E_\sigma^e = \tilde{\rho}_e^p E_0 \tag{3.12}$$

This is to prevent artificial modes in low density regions from dominating the solution while maintaining a continuous interpolation of element stiffness [15].

We choose to formulate the eigenvalue problem in terms of the reciprocal of the critical load for three reasons. The first is that $\mathbf{K}$ is guaranteed to be positive definite whereas $\mathbf{K}_\sigma$ is not, thus the proposed formulation enables the use of superior algorithms available for symmetric positive definite matrices such as methods based on Cholesky decomposition [32] or pre-conditioned conjugate gradient [33]. The second reason is that maximization of the smallest critical load is the objective, and optimization routines are formulated by default to minimize the objective. In this sense it is more practical to optimize the inverse of the critical loaded than the critical load itself. The third reason is that many eigenvalue routines, including the Implicitly Restarted Lanczos method [34] which we have used, converge more quickly to the largest eigenvalues [35]. Since we are most concerned with the smallest buckling loads, seeking the inverse of the smallest loads is computationally more efficient.

The sensitivities of the stability problem are more intricate computationally than any of the other functions. The formulation is described by [15]:

$$\frac{\partial \lambda_i}{\partial \rho_e} = \phi_i^T \left[\frac{\partial \mathbf{K}_\sigma(\mathbf{u})}{\partial \rho_e} - \lambda_i \frac{\partial \mathbf{K}}{\partial \rho_e} \right] \phi_i + \mathbf{v}_i^T \frac{\partial \mathbf{K}}{\partial \rho_e} \mathbf{u} \tag{3.13}$$

where $\mathbf{v}_i$ is the solution to the adjoint load problem

$$\mathbf{K}\mathbf{v}_i = \phi_i^T \frac{\partial \mathbf{K}_\sigma(\mathbf{u})}{\partial \mathbf{u}} \phi_i \tag{3.14}$$

A more detailed description of the implementation is available in the appendix.

In addition, some care must be taken to deal with multiplicity of eigenvalues. The formula for sensitivities is really only valid when the eigenvalue corresponding to the critical buckling load is simple. A rigorous method for adapting the sensitivity analysis in the event of multiple eigenvalues is presented by [36, 37]. A more typical approach, adopted here, is to use a

bound formulation [15] and simply restrict each consecutive eigenvalue to be a certain percent smaller than the previous eigenvalue:

$$\alpha^i \lambda_i \leq \beta \tag{3.15}$$

where α is some value slightly less than 1 (e.g. 0.99) and β is the objective value to be minimized. Thus, multiplicity of eigenvalues is restricted and differentiability of the critical eigenvalues is ensured.

3.2.4 Multi-Objective Function

To perform multi-objective optimization using MMA for the optimization updates, we follow the procedure outlined by Arora et [38] and Beghini [39]. First we normalize all of the objective functions using the following formula:

$$f_i^{norm} = \frac{f_i(\rho, \mathbf{u}(\rho)) - f_i^0}{f_i^{max} - f_i^0} \tag{3.16}$$

Where f_i^0 is the optimum obtained for objective function i alone and f_i^{max} is the maximum (furthest from optimal) value of objective function i alone. To determine f_i^0, we run independent trials for each objective function with all other criteria (domain, boundary conditions, filter, and constraints) remaining the same. The results of each independent trial give us the normalization factors for each objective function. However, since the maximum value of some functions such as compliance and stability can approach infinity, we instead use engineering intuition to cap f_i^{max} at some reasonable value.

Once we have normalized each of the functions, we use the weighted sum method to form a single objective function. To do this, we apply a weight, w_i, to each function, f_i, and then sum them together. By ensuring that $\sum w_i = 0$ and writing the multi-objective function as $f = \sum w_i f_i^{norm}(\rho, \mathbf{u}(\rho))$, we may determine the relative role of each objective function. The weights are initially chosen to give each objective function a relatively equal influence on the combined objective function. Adjusting the weights of each function yields different topologies. For example, setting the weight for the compliance function very high relative to the weights for the perimeter and buckling functions effectively yields the compliance minimization subject to a volume constraint that is frequently used in topology optimization. Some visual

examples of this follow in the results section.

CHAPTER 4

RESULTS

Applying compliance minimization with a volume constraint to this set of domain and boundary conditions produces the structure in Figure 4.1. As it is expected, the result is a structure with many thick columns merging into arches near the nodes where load is applied. Adding the perimeter function as a second objective with compliance modifies the topology to give thinner members, although the overall orientation of members remains unchanged. Figure 4.2 shows how the topology changes with increasing or decreasing emphasis on the perimeter function. The general trend is that increasing the emphasis on the perimeter function will lead to more, thinner members in the final result. While this is relatively unimportant from a structural perspective, the increased surface area is highly advantageous from a biological perspective. Such perforated structures are common, for instance, in trabecular bone where repairs to damaged bone are performed on the surface [30].

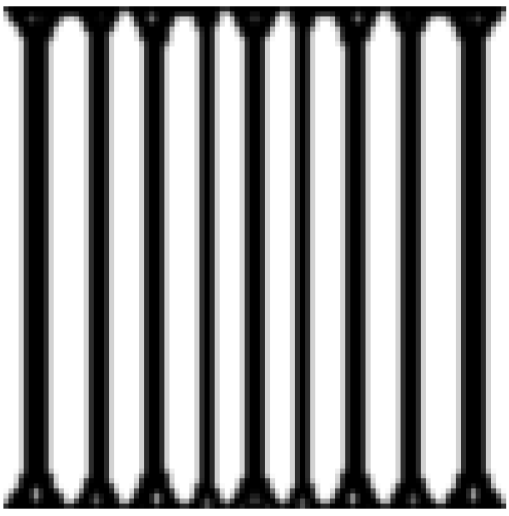

Figure 4.1: Optimal structure corresponding to compliance minimization subjected to a volume constraint = 0.4.

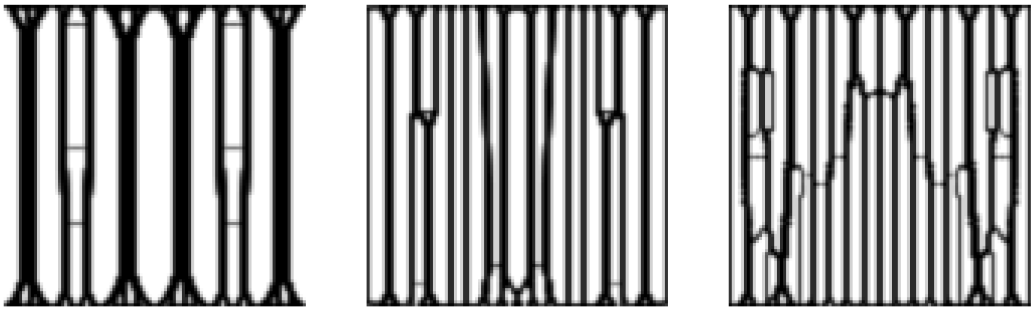

(a) Compliance weight = 99.999% and perimeter weight = 0.001%.

(b) Compliance weight = 99.9% and perimeter weight = 0.1%.

(c) Compliance weight = 95% and perimeter weight = 5%.

Figure 4.2: Multi-objective formulation with varying weights on compliance and perimeter functions to show the effects of the perimeter function. All cases have a volume constraint = 0.4. The optimized compliance value is 27.4% higher in b (0.129 N*mm) than in a ($0.102N\ mm$), and it is 14.3% higher in c ($0.148N\ mm$) than in b.

Figure 4.3 demonstrates the interaction of stability with the compliance and perimeter functions. In Figure 4.3a, the compliance part of the objective motivates the development of thick columns, while the stability consideration leads to the development of diagonal members to increase the critical buckling load. In Figure 4.3b, the perimeter part of the objective motivates the development of many small voids and a lot of thin members, while the optimization of stability pushes the members to orient in a pattern that inhibits buckling. These images, combined with the results in Figure 4.2 serve to demonstrate that any two of these functions alone are not sufficient to develop the intricate structure we are looking for. Without stability there is no motivation for significant non-vertical members, without the perimeter function, the created members are too thick, and without compliance, nearly all the resulting members are diagonal.

Applying compliance, perimeter, and critical buckling load as multiple objectives with varying weights for each yields the results in Figure 4.4. While the previous optimization problem resulted in structures dominated by vertical lines, the inclusion of stability here and previously in Figure 4.3 leads to a much more intricate structure with many non-vertical members. However, the resulting structure can vary widely depending on the relative weight of each function. Higher emphasis on perimeter leads to a larger number of voids and smaller members. Contrarily, reducing the emphasis on perime-

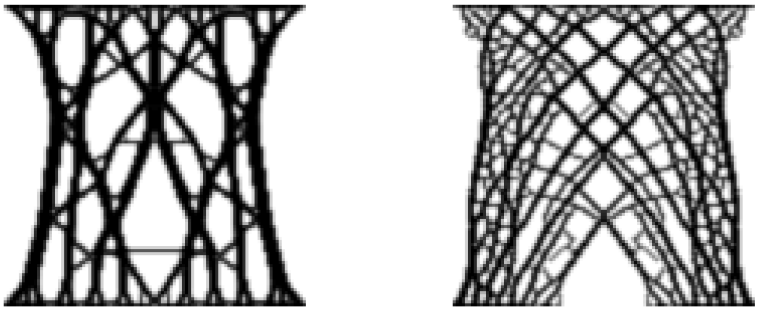

(a) Compliance weight = 50% and stability weight = 50%.

(b) Perimeter weight = 10% and stability weight = 90%.

Figure 4.3: Multi-objective formulation displaying the effects of the stability function.

ter leads to an increase in the size of voids and a thickening of members. Increasing the weight of compliance leads the structure to form primarily vertical members, while reducing it leads to the development of mostly diagonal members. Finally, emphasizing stability leads to the development of more and thicker non-vertical members, while deemphasizing it leads to primarily vertical members. When the influence of the perimeter function is small, these non-vertical members are often diagonal, as would be the case in a braced frame. However, with increasing weight on perimeter, these members become more horizontal (orthogonal to the other members), as in the case of trabecular bone. Interestingly, the models with higher emphasis on stability relative to compliance also appear to contribute to curvature along the sides of the domain, similar to the geometry of the vertebral body. Overemphasizing perimeter also contributes to the development of isolated, non-connected members that serve no mechanical purpose. By tuning the weights of different objectives, a structure very similar to vertebral trabecular bone begins to emerge (Figure 4.4b).

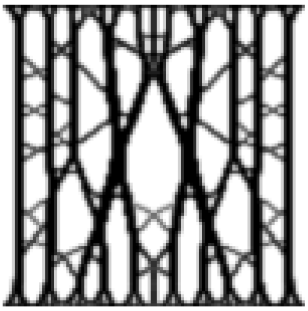

(a) Compliance weight = 86.9%, perimeter weight = 0.1%, and stability weight = 13%.

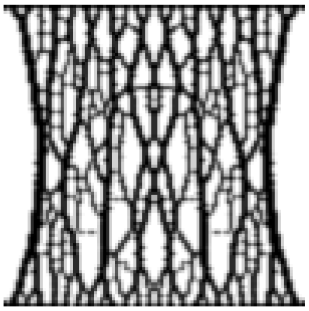

(b) Compliance weight = 75%, perimeter weight = 20%, and stability weight = 5%.

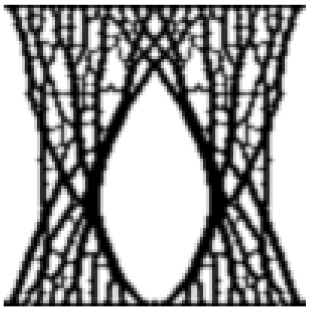

(c) Compliance weight = 60%, perimeter weight = 20%, and stability weight = 20%.

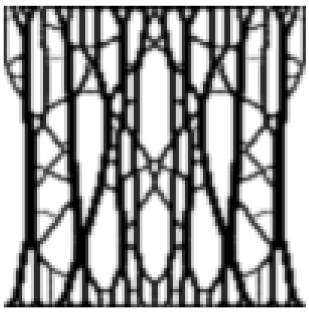

(d) Compliance weight = 90%, perimeter weight = 5%, and stability weight = 5%.

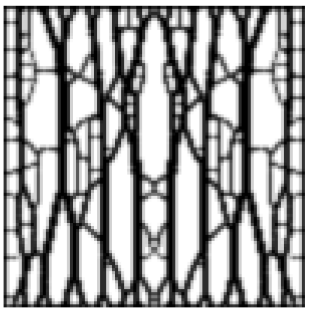

(e) Compliance weight = 88%, perimeter weight = 10%, and stability weight = 2%.

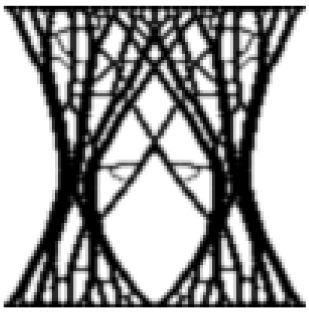

(f) Compliance weight = 60%, perimeter weight = 10%, and stability weight = 30%.

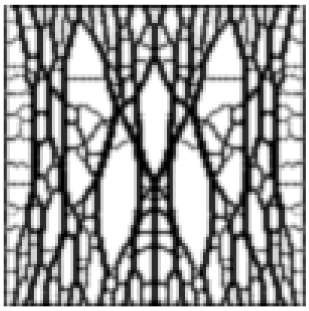

(g) Compliance weight = 80%, perimeter weight = 10%, and stability weight = 10%.

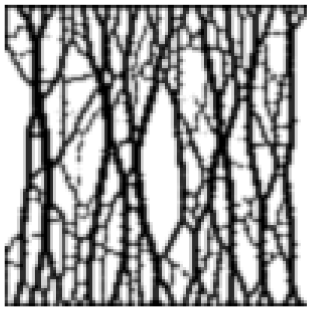

(h) Compliance weight = 75%, perimeter weight = 20%, and stability weight = 5%.

Figure 4.4: Optimized structure for various combinations of all three objective functions. All Figures have volume fraction = 0.4 and all except h have symmetry enforced.

CHAPTER 5

DISCUSSION

In this paper, we have investigated the evolution of trabecular structure in a 2D model of a vertebral body using a multi-objective topology optimization framework. We use a weighted sum formulation to combine compliance, surface area and buckling strength as objective functions and we use a constraint on the volume fraction. Our primary result is that the combination of these three different objectives, within the context of a simple bone plate model, is essential to reproduce the intricate structure of the vertebral body when it is loaded predominantly by vertical loads. In particular, without considerations of stability the resulting structures deviate significantly from the tomographic scans of real trabecular bone and may be vulnerable to buckling.

5.1 Multi-Objective vs. Multiple Constraints

Topology optimization with a single objective and multiple constraints has been explored extensively, and can produce excellent results, including applications of biomimicry [5, 6, 16]. However, we believe it is more consistent with the underlying biology to combine several functions into an overarching objective function. In this sense, there are no invalid (constraint violating) designs, but instead the formulation can increase the influence of a particular function (e.g. compliance) by weighing it more heavily in the combined objective function. This system of weights reflects the shifting importance of biological roles over time and could be used to mimic the effects of age or disease.

In using a weighted sum multi-objective approach as opposed to a single objective with multiple constraints we have been able to explore the relative role of compliance, surface area, and stability in determining the trabecular

structure. The approach also enables us to investigate the variability in the resulting design as a function of changes in the relative weight of the different objectives. This may be relevant in future design of smart and programmable materials which will possess an ability to morph or adapt to meet specific objectives. The flexibility of the weighted sum approach also allows us to treat the topology optimization as an inverse analysis method. In this setting, we construct a problem where the weights are optimized to minimize the difference between an observed structure and the resulting topology, similar to what we have done in this paper.

While at face value the weight factors used may indicate that compliance is essential to development of the trabecular-like structures and perimeter is in some cases a trivial consideration, this is may not be true. While the use of this weighted sum approach does provide an effective way for us to combine the objective functions, the weights themselves do not provide a well-determined evaluation of the influence of each objective function. Rather, factors such as the method used to normalize the objective functions are just as important in influencing the structure. We present our results in the following section by specifying the weights used for each objective function to characterize the resulting shapes as it is consistent with the multi-objective formula we presented earlier. However, we would like to clarify that these weights are only accurate if using the same normalization method we described. If the functions are normalized in a different manner, then different weights are necessary. Thus, we ask that the reader regard these weights as only relative factors and not sufficient by themselves to create a specific structure. Accordingly, saying that a weight of 99% was used for a specific objective would not indicate that this objective is 99% responsible for the resulting structure, it simply indicates that this objective plays a more important role in determining the structure than if a weight of 90% was used, for example. The weights are highly dependent on the normalization method used and are only truly valid to compare the influence of the same function in different models. For example in Figure 4.4d, the compliance function doesnt necessarily account for 90% of the resulting structure nor is it strictly 18 times more influential than perimeter or stability. However, it is true that the compliance function is much more influential in Figure 4.4d, than it is in Figure 4.4c, (which should be apparent from the resulting structure).

A point of departure in this paper from previous work (e.g. [6]) is that we

investigate the perimeter as part of the objective function. This is motivated by the idea that the perimeter value appropriate for a specific biological structure may not be a priori known and may vary widely even if the volume fraction is known. Hence we think that imposing the perimeter as a constraint may restrict the design space. We have also expanded the formulation by including additional considerations of stability. It would of course be possible to incorporate all of these functions into a single formulation by picking one as an objective and assigning the rest as constraints [5, 6, 16]. However, this would require determining a constraint value for each function, which is non-trivial and more importantly may unnecessarily restrict the design space, which is already non-convex.

The results of this multi-objective formulation also warrant further investigation with volume included as part of the objective rather than a constraint. In such a formulation, there would be no conventional constraint, but rather the resulting structure could be controlled by adjusting the weight factors for each individual objective. This would be particularly appealing from a biological perspective, where factors such as age or disease may make bone material more expensive. Rather than prescribing a set volume fraction, it would be possible to increase or decrease the relative weight of volume to simulate changes in metabolic rates, among other factors. Some preliminary work on this idea is included in the appendix.

Our current formulation still requires setting a weight for each function, but the weights are only relative to each other. Thus we do not need to determine biologically-derived values for constraints, but rather a relative effect of each role. While the weights do have a significant impact on the resulting structure, they are also less restrictive than constraints which may greatly reduce the available design space. Consequently, we hypothesize that the multi-objective approach is a better representation of the processes that determine the formation of trabecular bone, where the structure must serve different roles as best as possible. While many man-made structures may have preset design values, biological structures must be free to adapt to changing boundary conditions or increased importance of certain biological roles. However, the list of objective functions introduced here is not exhaustive. Many other functions, such as flaw tolerance, fracture arrest, or conductivity, may be included. The presented multi-objective approach is intended to be flexible enough to incorporate any number of these functions.

5.2 Stability Problem

By modeling the domain with a uniform mesh of elements, we were able to include the stability problem with little extra cost aside from the eigenvalue solver. Given that the eigenvalue problem accounts for more than 50% of total computation time in the stability problem, considering stability is only marginally more expensive than other problems, such as those involving modal analysis, which have received more attention in the context of topology optimization. Given that much work has been done in stress or compliance minimization problems, while neglecting instabilities that may arise, it is our hope that this work will also contribute to the wider consideration of stability in topology optimization in general and bio-inspired design in particular.

Unfortunately, the cost of the eigenvalue problem is still quite formidable. The best method for this problem, the implicitly restarted Lanczos algorithm [34], requires repeated solutions of a linear system with high accuracy, which is only feasible with a factorization of the matrix. For large scale computations, a factorization becomes difficult, and it is particularly inefficient in a parallel implementation. The Davidson or Jacobi-Davidson method [40] is much better suited for large scale and parallel implementations since it only requires iterative solutions with relatively low accuracy. However, these methods are better suited for problems with clustered eigenvalues, and have displayed poor convergence for the stability problem considered here. There is a need to develop an efficient method to repeatedly solve the generalized eigenvalue problem at a large scale during the optimization process. Developing such techniques is part of our ongoing efforts in tackling these problems. Given the aforementioned similarity between stability and dynamics problems, other approaches such as multiresolution topology optimization could also provide significant improvements [41].

5.3 Domain and Filtering

In this paper, we have assumed a simple rectangular geometry for the vertebral domain as well as uniform loading and support conditions. The effect of deterioration in the intervertebral discs may be modeled by adjusting the distribution of load across the top. Healthy discs tend to have high

compressive loads in the interior of the disc and lighter compressive or tensile loads near the edge of the disc. As the discs age or degrade, compressive load in the center begins to decrease and compressive loads near the exterior begin to increase to the point that little to no load is transferred through the interior [8]. In that sense, our model closely represents a healthy end condition. Further exploration of the effect of these changing conditions due to age and disease will be the subject of a future work.

For the purposes of this paper, we have implemented a linear density filter to alleviate some of the issues that arise with the use of low-order elements, such as checkerboarding. Several alternatives to the density filter exist, although it would be difficult to say that one is clearly better than any of the others. The most common alternative is a sensitivity filter [42, 43, 44], where the element density is unchanged ($\tilde{\rho} = \rho$), and the sensitivities are filtered directly. The theory behind this form of filter is less rigorously developed than that of the density filter and presents inherent risks (filtered sensitivities may not represent a descent direction), but has been shown to be very robust in practice. Another, less common alternative is to use higher-order elements in the mesh. This could be done by increasing the polynomial order but retaining the same element shape (e.g. Q8 elements) or by using polygonal elements [45]. However, the use of higher order elements increases the cost of the FE problem, and in the case of polygonal elements we lose the regularity of the mesh. This is of particular importance in the perimeter and stability functions where the use of identical elements provides significant advantages in the sensitivity formulations. However, these higher order methods remain an attractive alternative due to their robustness despite some algorithmic complexities.

We have also imposed symmetry in the design as described by Kosaka and Swan [46]. Despite the perfect symmetry of the domain and boundary conditions, we have found that it is very difficult to produce perfect symmetry in the design results for a number of reasons. The simplest reason for this is that the uniformity of the boundary conditions worsens the conditioning of the problem and therefore increases susceptibility to numerical errors. It is possible to overcome this issue by carefully setting optimization parameters, particularly within the MMA routine, but this is an inefficient solution as the necessary parameters change if any part of the problem changes (e.g. objective or constraint function, convergence tolerance, filter size, etc.). In

addition, the stability function introduces additional asymmetry that cannot as easily be controlled. In particular, the eigenvalue problem cannot assume symmetry as buckling modes are rarely symmetric and thus the iterative eigensolver generally introduces additional asymmetry through the associated sensitivities. By using symmetry in the design and not in the analysis, we are able ensure our results are symmetric without any of the compromises that would come with optimizing on a symmetric domain (e.g. obscuring non-symmetric buckling modes).

5.4 Future Work

Future extension of this work may include exploring the effect of changing boundary conditions, particularly the degradation of intervertebral discs as mentioned previously. The thinning of trabecular bone with age has been well documented [47] and it is possible that redistribution of external loads plays some part in this. In addition, we can apply the formulation to different parts of the body, particularly the proximal femur, to explore how different parts of the body adapt to applied boundary conditions. Investigating the proximal femur will also allow us to compare our work more directly to existing results [5, 6]. Another possible direction for future work is the exploration of hierarchical topology optimization as in Rodrigues et al. [48], where we allow for material anisotropy at the macroscale by simultaneously optimizing a microstructure.

From a biomedical perspective, this approach may enable us to produce individualized scaffolds to rebuild or replace damaged bones through additive manufacturing techniques. Some pioneering work has already been done using topology optimization as a framework to repair bones [49]. We believe our current formulation expands on this and encompasses additional complexities associated with the many biological functions bone must serve. It may also open new opportunities in a variety of medical and structural applications.

CHAPTER 6

CONCLUSION

- We have used multi-objective topology optimization to replicate some of the key features of trabecular bone in the vertebral body.
- Our model is the first to analyze trabecular bone structure while considering the effects of stability. Numerous previous analyses have only considered compliance, surface area (perimeter), and volume. The consideration of perimeter in these designs makes the resulting structures inherently prone to instabilities by reducing the average member size.
- Using a multi-objective approach also presents us with increased flexibility in optimizing structures. Rather than reducing the feasible design space, we can adjust the function weights to produce structures that are more or less favorable in certain applications.
- For example, increasing the role of surface area or perimeter makes structures more appealing in biomimetic applications, while increasing the role of stiffness will produce structures more in line with conventional engineering practices.
- Our results have also shown that placing slightly more emphasis on compliance and less emphasis on stability produced the results most similar to real trabecular bone.
- The finite element model used was a simplified rectangular representation of the vertebral body with 10,000 elements consistent with the plate model of bone. Going forward, we would like to be able to incorporate a larger number of elements, but the expense of the eigenvalue problem for stability makes a large number of elements exceedingly expensive in the current approach.

- The eigenvalue problem is poorly-suited for implementation in a parallel application, and other methods for increasing the discretization are likely to be more effective.
- One possibility is using multiresolution topology optimization to increase the number of design variables without significantly increasing the number of elements in the finite element model.
- Fortunately, the cost of this formulation outside of the eigenvalue problem remains relatively small, so any strategy that reduces the cost of the finite element problem relative to the optimization problem will be very effective in enabling greater discretization of the design problem.

Appendices

APPENDIX A

STABILITY SENSITIVITIES

Carefully implementing the sensitivity calculations for the stability problem is crucial in making the code run efficiently. Solving either the adjoint problem or the total sensitivity formulation using sparse matrices to represent $\partial \mathbf{K}/\partial \rho_e$ and $\partial \mathbf{K}_\sigma/\partial \rho_e$ is prohibitively expensive. In fact, using sparse matrix operations increases the compute time to more than an order of magnitude greater than the rest of the optimization problem combined. It is instead several orders of magnitude quicker to recognize that both of these quantities are essentially dense square matrices with a specific size, n_{dof} number of degrees of freedom per element, and use dense matrix operations.

Using this methodology, the sensitivities can be constructed in two efficient loops over all the elements. The first loop constructs the vector $\phi_i^T \left[\partial \mathbf{K}_\sigma(\mathbf{u})/\partial \mathbf{u}\right] \phi_i$ by adding each elements contributions to the appropriate index of the global array. Since we are using a uniform mesh of elements, we can speed up computations by calculating the sensitivity of the local stress stiffness matrix with respect to a change in displacement and normalized by the element stiffness:

$$\frac{1}{E_\sigma^e} \frac{\partial \mathbf{k}_\sigma(\mathbf{u})}{\partial \mathbf{u}} \tag{A.1}$$

This only has to be done once and results in a fully dense 3D array with size n_{dof} in each dimension. In our implementation we have further modified it to treat each slice of the sensitivity array as a vector and perform all subsequent matrix operations as vector operations, although this is not strictly necessary from a performance perspective. Then at each iteration, a loop simply pre and post multiplies (A.1) by the local component of the eigenvector (denoted here as ϕ_i) and multiplies the resulting scalar by E_σ^e. This value is then added to the appropriate index of the global vector. Thus, the right-hand-side vector in the adjoint problem is just:

$$\sum_{e=1}^{n_{el}} \sum_{r=1}^{n_{dof}} E_\sigma^e \phi_i^T \frac{1}{E_\sigma^e} \frac{\partial \mathbf{k}_{pq}^\sigma}{\partial \mathbf{u}_r} \phi_i \tag{A.2}$$

After solving the linear system to determine $\mathbf{v}_i$, another loop constructs $\partial\lambda_i/\partial\rho_e$ element by element. Here again it is important to note that the calculation of $\partial\lambda_i/\partial\rho_e$ only requires the local parts of ϕ_i, $\mathbf{v}_i$, and $\mathbf{u}_i$ in order to make the computations efficient. This second loop combines the partial sensitivities of the two matrices $\mathbf{K}$ and $\mathbf{K}_\sigma$ with the solution to the adjoint problem:

$$\phi_i^T \left[\frac{\partial \mathbf{K}_\sigma}{\partial \rho_e} - \lambda_i \frac{\partial \mathbf{K}}{\partial \rho_e} \right] \phi_i + \mathbf{v}_i \frac{\partial \mathbf{K}}{\partial \rho_e} \mathbf{u} \tag{A.3}$$

In this formula, everything has already been calculated and stored known apart from the matrix partial sensitivities. Fortunately, these are trivial to calculate. The sensitivities of the local part of the matrix $\mathbf{K}$ are:

$$\frac{\partial \mathbf{k}}{\partial \rho_e} = \frac{\partial E_e}{\partial \rho_e} \int_{\Omega_e} \mathbf{B}^T \mathbf{D} \mathbf{B} dv \tag{A.4}$$

and the sensitivities of the local part of the $\mathbf{K}_\sigma$ are similarly:

$$\frac{\partial \mathbf{k}_\sigma}{\partial \rho_e} = \frac{\partial E_\sigma^e}{\partial \rho_e} \int_{\Omega_e} \mathbf{G}^T \mathbf{S} \mathbf{G} dv \tag{A.5}$$

The integrals in (A.4) and (A.5) will have already been calculated in order to construct the $\mathbf{K}$ or $\mathbf{K}_\sigma$ matrices. This means that the only operations necessary to construct the terms inside the brackets in (A.3) are a scalar times a matrix ($\lambda_i \cdot \partial\mathbf{K}/\partial\rho_e$) and the subtraction of two matrices. Given that all of the work in the sensitivity calculation is local except for the solution of the adjoint problem, the entire algorithm also parallelizes very nicely.

APPENDIX B

UNCONSTRAINED OPTIMIZATION

To demonstrate the validity of applying topology optimization without a conventional constraint (we still use constraints on eigenvalue distinctness as part of the aforementioned bound formulation), we present an optimized design with compliance, perimeter, volume, and stability all as objective functions. By inspection, it appears that Figure B.1 shares many qualitative similarities with the images in Figure 4.4, in particular Figure 4.4g. We believe that by incorporating all of the functions as part of a multi-objective formulation we will provide greater flexibility in mimicking the changing importance of biological roles in applications of biomimicry.

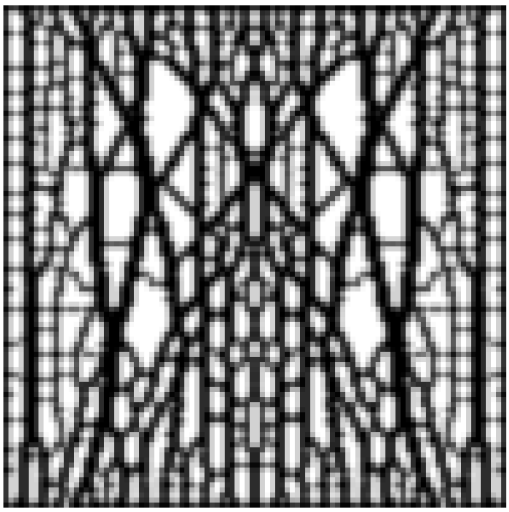

Figure B.1: Unconstrained optimization result.

APPENDIX C

SYMMETRY

For the results presented in this paper, we have enforced symmetry of the design since the domain and boundary conditions are both symmetric. However, from a theoretical standpoint, the enforcement of symmetry should not be strictly necessary, as the choice of domain, boundary conditions, objective functions, and constraint functions should produce a symmetric design. In the case of the simple compliance minimization with volume constraint problem, this is usually the case, as long as move limits are kept small (0.2 or less). Trouble arises when either the perimeter function is included or the move limits are set too high (1.0). In this case, numerical artifacts (non-differentiability of the perimeter function at edges where elements have equal densities or small numerical errors in the calculation of sensitivities) can artificially push the design to one of asymmetry. While a true global optimum would likely require a symmetric design, these asymmetric designs represent local minima that are only marginally worse than the true global optimum. As a result, asymmetric designs are common in the multi-objective case and it is more prudent to enforce design symmetry than to try and ascertain the proper move limits to ensure symmetry while allowing the optimization to converge reasonably quickly. In our experience, enforcing design symmetry also produced better optimum values than reducing the move limit, although there is no guarantee that this effect will always be observed.

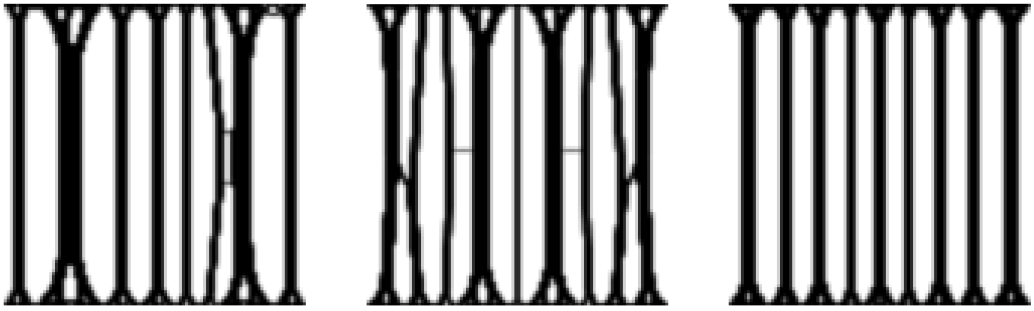

(a) No enforced symmetrization with move limit = 1.0 (Compliance = 0.1006).

(b) No enforced symmetrization and move limit = 0.2 (Compliance = 0.1071).

(c) Enforced symmetry in the design and move limit = 1.0 (Compliance=0.09985).

Figure C.1: Optimal structures resulting from a problem with compliance minimization and a volume constraint.

REFERENCES

[1] I. Parkinson and N. Fazzalari, "Characterisation of Trabecular Bone Structure," in *Skeletal Aging and Osteoporosis*, ser. Studies in Mechanobiology, Tissue Engineering and Biomaterials, M. J. Silva, Ed. Springer Berlin Heidelberg, jan 2013, vol. 5, pp. 31–51. [Online]. Available: http://dx.doi.org/10.1007/8415_2011_113

[2] G. H. Meyer, "Archief fur den anatomische und physiologischen Wissenschaften im Medizin," *Die Architektur der Spongiosa*, no. 34, pp. 615–628, 1867.

[3] K. Culmann, *Die graphische Statik*. Meyer & Zeller, Zurich, Switzerland, 1866. [Online]. Available: https://books.google.com/books?id=Ab8KAAAAIAAJ

[4] J. Wolff, *Das Gesetz der Transformation der Knochen*. Pro Business, 2010. [Online]. Available: http://books.google.com/books?id=CixTtwAACAAJ

[5] C. Boyle and I. Y. Kim, "Three-dimensional micro-level computational study of Wolff's law via trabecular bone remodeling in the human proximal femur using design space topology optimization," *Journal of Biomechanics*, vol. 44, no. 5, pp. 935–942, mar 2011. [Online]. Available: http://www.sciencedirect.com/science/article/pii/S002192901000655X

[6] I. G. Jang and I. Y. Kim, "Computational study of Wolff's law with trabecular architecture in the human proximal femur using topology optimization," *Journal of Biomechanics*, vol. 41, no. 11, pp. 2353–2361, aug 2008. [Online]. Available: http://www.sciencedirect.com/science/article/pii/S0021929008002807

[7] R. B. Haber, C. S. Jog, and M. P. Bendsøe, "A new approach to variable-topology shape design using a constraint on perimeter," *Structural Optimization*, vol. 11, no. 1-2, pp. 1–12, jan 1996. [Online]. Available: http://dx.doi.org/10.1007/BF01279647

[8] D. G. Orndorff, M. A. Scott, and K. A. Patty, "Force Transfer in the Spine," *Journal of the Spinal Research Foundation*, vol. 7, no. 2, pp. 30–35, 2012.

[9] M. M. Neves, H. Rodrigues, and J. M. Guedes, "Generalized topology design of structures with a buckling load criterion," *Structural Optimization*, vol. 10, no. 2, pp. 71–78, jan 1995. [Online]. Available: http://dx.doi.org/10.1007/BF01743533

[10] S. Min and N. Kikuchi, "Optimal reinforcement design of structures under the buckling load using the homogenization design method," *Structural Engineering and Mechanics*, vol. 5, no. 5, pp. 565–576, 1997.

[11] H.-C. Cheng, K.-N. Chiang, and T.-Y. Chen, "Optimal configuration design of elastic structures for stability," in *High Performance Computing in the Asia-Pacific Region, 2000. Proceedings. The Fourth International Conference/Exhibition on*, vol. 2, 2000, pp. 1112–1117 vol.2.

[12] B.-c. Bian and Y.-k. Sui, "Topology Optimization of Continuum Structures under Buckling and Displacement Constraints," in *2009 International Conference on Information Technology and Computer Science*, vol. 2. IEEE, jul 2009. [Online]. Available: http://ieeexplore.ieee.org/lpdocs/epic03/wrapper.htm?arnumber=5190268 pp. 417–420.

[13] P. A. Browne, C. Budd, N. I. M. Gould, H. A. Kim, and J. A. Scott, "A fast method for binary programming using first-order derivatives, with application to topology optimization with buckling constraints," *International Journal for Numerical Methods in Engineering*, vol. 92, no. 12, pp. 1026–1043, 2012. [Online]. Available: http://dx.doi.org/10.1002/nme.4367

[14] E. Lindgaard and J. Dahl, "On compliance and buckling objective functions in topology optimization of snap-through problems," *Structural and Multidisciplinary Optimization*, vol. 47, no. 3, pp. 409–421, jan 2013. [Online]. Available: http://dx.doi.org/10.1007/s00158-012-0832-2

[15] M. P. Bendsøe and O. Sigmund, *Topology Optimization: Theory, Methods and Applications*, ser. Engineering online library. Springer, 2003. [Online]. Available: http://books.google.com/books?id=NGmtmMhVe2sC

[16] I. G. Jang and I. Y. Kim, "Computational study on the effect of loading alteration caused by disc degeneration on the trabecular architecture in human lumbar spine," *Journal of Biomechanics*, vol. 43, no. 3, pp. 492–499, feb 2010. [Online]. Available: http://www.sciencedirect.com/science/article/pii/S0021929009005612

[17] O. Sigmund, "On the usefulness of non-gradient approaches in topology optimization," *Structural and Multidisciplinary Optimization*, vol. 43, no. 5, pp. 589–596, jan 2011. [Online]. Available: http://dx.doi.org/10.1007/s00158-011-0638-7

[18] M. P. Bendsøe, A. Díaz, and N. Kikuchi, "Topology and Generalized Layout Optimization of Elastic Structures," in *Topology Design of Structures*, ser. NATO ASI Series, M. P. Bendsøe and C. A. M. Soares, Eds. Springer Netherlands, jan 1993, vol. 227, pp. 159–205. [Online]. Available: http://dx.doi.org/10.1007/978-94-011-1804-0_13

[19] T. E. Bruns and D. A. Tortorelli, "Topology optimization of non-linear elastic structures and compliant mechanisms," *Computer Methods in Applied Mechanics and Engineering*, vol. 190, no. 2627, pp. 3443–3459, 2001. [Online]. Available: http://www.sciencedirect.com/science/article/pii/S0045782500002784

[20] K. Svanberg and H. Svärd, "Density filters for topology optimization based on the Pythagorean means," *Structural and Multidisciplinary Optimization*, vol. 48, no. 5, pp. 859–875, jan 2013. [Online]. Available: http://dx.doi.org/10.1007/s00158-013-0938-1

[21] M. P. Bendsøe and O. Sigmund, "Material interpolation schemes in topology optimization," *Archive of Applied Mechanics*, vol. 69, no. 9-10, pp. 635–654, jan 1999. [Online]. Available: http://dx.doi.org/10.1007/s004190050248

[22] M. P. Bendsøe, "Optimal shape design as a material distribution problem," *Structural Optimization*, vol. 1, no. 4, pp. 193–202, jan 1989. [Online]. Available: http://dx.doi.org/10.1007/BF01650949

[23] M. Stolpe and K. Svanberg, "On the trajectories of penalization methods for topology optimization," *Structural and Multidisciplinary Optimization*, vol. 21, no. 2, pp. 128–139, jan 2001. [Online]. Available: http://dx.doi.org/10.1007/s001580050177

[24] K. Svanberg, "The method of moving asymptotes-a new method for structural optimization," *International Journal for Numerical Methods in Engineering*, vol. 24, no. 2, pp. 359–373, 1987. [Online]. Available: http://dx.doi.org/10.1002/nme.1620240207

[25] I. G. Jang, I. Y. Kim, and B. B. Kwak, "Analogy of strain energy density based bone-remodeling algorithm and structural topology optimization." *Journal of biomechanical engineering*, vol. 131, no. 1, p. 011012, jan 2009. [Online]. Available: http://biomechanical.asmedigitalcollection.asme.org/article.aspx?articleid=1475625

[26] M. Mullender, R. Huiskes, and H. Weinans, "A physiological approach to the simulation of bone remodeling as a self-organizational control process," *Journal of Biomechanics*, vol. 27, no. 11, pp. 1389–1394, nov 1994. [Online]. Available: http://www.sciencedirect.com/science/article/pii/0021929094900493

[27] H. Weinans, R. Huiskes, and H. J. Grootenboer, "The behavior of adaptive bone-remodeling simulation models." *Journal of biomechanics*, vol. 25, no. 12, pp. 1425–41, dec 1992. [Online]. Available: http://www.ncbi.nlm.nih.gov/pubmed/1491020

[28] M. P. Bendsøe and N. Kikuchi, "Generating optimal topologies in structural design using a homogenization method," *Computer Methods in Applied Mechanics and Engineering*, vol. 71, no. 2, pp. 197–224, 1988. [Online]. Available: http://www.sciencedirect.com/science/article/pii/0045782588900862

[29] A. G. Robling, A. B. Castillo, and C. H. Turner, "BIOMECHANICAL AND MOLECULAR REGULATION OF BONE REMODELING," *Annual Review of Biomedical Engineering*, vol. 8, no. 1, pp. 455–498, 2006. [Online]. Available: http://dx.doi.org/10.1146/annurev.bioeng.8.061505.095721

[30] E. Seeman and P. D. Delmas, "Bone Quality The Material and Structural Basis of Bone Strength and Fragility," *N Engl J Med*, vol. 354, no. 21, pp. 2250–2261, 2006. [Online]. Available: http://dx.doi.org/10.1056/NEJMra053077

[31] R. D. Cook, D. S. Malkus, M. E. Plesha, and R. J. Witt, *Concepts and applications of finite element analysis*. Wiley, 2001, vol. 4th. [Online]. Available: https://books.google.com/books?id=b8seAQAAIAAJ

[32] W. H. Press, S. A. Teukolsky, W. T. Vetterling, and B. P. Flannery, *Numerical Recipes 3rd Edition: The Art of Scientific Computing*. Cambridge University Press, 2007, vol. 3rd. [Online]. Available: https://books.google.com/books?id=1aAOdzK3FegC

[33] M. R. Hestenes and E. Stiefel, "Methods of Conjugate Gradients for Solving Linear Systems," *Journal of Research of the National Bureau of Standards*, vol. 49, no. 6, pp. 409–436, 1952.

[34] D. C. Sorensen, "Implicitly Restarted Arnoldi/Lanczos Methods for Large Scale Eigenvalue Calculations," in *Parallel Numerical Algorithms*, ser. ICASE/LaRC Interdisciplinary Series in Science and Engineering, D. Keyes, A. Sameh, and V. Venkatakrishnan, Eds. Springer Netherlands, jan 1997, vol. 4, pp. 119–165. [Online]. Available: http://dx.doi.org/10.1007/978-94-011-5412-3_5

[35] M. T. Heath, *Scientific Computing: An Introductory Survey*, E. M. Munson, Ed. McGraw-Hill Higher Education, 2002, vol. 2nd.

[36] A. P. Seyranian, "Sensitivity Analysis of Multiple Eigenvalues*," *Mechanics of Structures and Machines*, vol. 21, no. 2, pp. 261–284, jan 1993. [Online]. Available: http://dx.doi.org/10.1080/08905459308905189

[37] A. P. Seyranian, E. Lund, and N. Olhoff, "Multiple eigenvalues in structural optimization problems," *Structural Optimization*, vol. 8, no. 4, pp. 207–227, dec 1994. [Online]. Available: http://link.springer.com/10.1007/BF01742705

[38] J. S. Arora, *Introduction to Optimum Design*. Elsevier, 2012. [Online]. Available: http://www.sciencedirect.com/science/article/pii/B9780123813756000176

[39] L. L. Beghini, "Building Science Through Topology Optimization," Ph.D. dissertation, Urbana, Illinois, 2013.

[40] G. L. G. Sleijpen and H. A. Van der Vorst, "A Jacobi–Davidson Iteration Method for Linear Eigenvalue Problems," *SIAM Review*, vol. 42, no. 2, pp. 267–293, jan 2000. [Online]. Available: http://epubs.siam.org/doi/abs/10.1137/S0036144599363084

[41] E. T. Filipov, J. Chun, G. H. Paulino, and J. Song, "Polygonal multiresolution topology optimization (PolyMTOP) for structural dynamics," *Structural and Multidisciplinary Optimization*, nov 2015. [Online]. Available: http://link.springer.com/10.1007/s00158-015-1309-x

[42] O. Sigmund, "Design of material structures using topology optimization." Ph.D. dissertation, DK-2800 Lyngby, the Danish Center for Applied Mathematics and Mechanics, 1994.

[43] O. Sigmund, "On the Design of Compliant Mechanisms Using Topology Optimization," *Mechanics of Structures and Machines*, vol. 25, no. 4, pp. 493–524, 1997. [Online]. Available: http://dx.doi.org/10.1080/08905459708945415

[44] O. Sigmund and J. Petersson, "Numerical instabilities in topology optimization: A survey on procedures dealing with checkerboards, mesh-dependencies and local minima," *Structural Optimization*, vol. 16, no. 1, pp. 68–75, jan 1998. [Online]. Available: http://dx.doi.org/10.1007/BF01214002

[45] C. Talischi, G. Paulino, A. Pereira, and I. M. Menezes, "PolyTop: a Matlab implementation of a general topology optimization framework using unstructured polygonal finite element meshes," *Structural and Multidisciplinary Optimization*, vol. 45, no. 3, pp. 329–357, jan 2012. [Online]. Available: http://dx.doi.org/10.1007/s00158-011-0696-x

[46] I. Kosaka and C. C. Swan, "A symmetry reduction method for continuum structural topology optimization," *Computers & Structures*, vol. 70, no. 1, pp. 47–61, jan 1999. [Online]. Available: http://www.sciencedirect.com/science/article/pii/S0045794998001588

[47] R. O. Ritchie, M. J. Buehler, and P. Hansma, "Plasticity and toughness in bone," *Physics Today*, pp. 41–47, 2009.

[48] H. Rodrigues, C. Jacobs, J. M. Guedes, and M. P. Bendsøe, "Global and Local Material Optimization Models Applied to Anisotropic Bone Adaptation," in *IUTAM Symposium on Synthesis in Bio Solid Mechanics*, ser. Solid Mechanics and its Applications, P. Pedersen and M. P. Bendsøe, Eds. Springer Netherlands, jan 2002, vol. 69, pp. 209–220. [Online]. Available: http://dx.doi.org/10.1007/0-306-46939-1_19

[49] A. Sutradhar, G. Paulino, M. J. Miller, and T. H. Nguyen, "Topological optimization for designing patient-specific large craniofacial segmental bone replacements," *Proceedings of the National Academy of Sciences of the United States of America*, vol. 107, no. 30, pp. 13 222–13 227, 2010.